

Rotational dynamics of dissociating H_2^+ in a short intense laser pulse

This article has been downloaded from IOPscience. Please scroll down to see the full text article.

2009 J. Phys. B: At. Mol. Opt. Phys. 42 091001

(<http://iopscience.iop.org/0953-4075/42/9/091001>)

View [the table of contents for this issue](#), or go to the [journal homepage](#) for more

Download details:

IP Address: 38.107.179.212

The article was downloaded on 21/02/2012 at 13:09

Please note that [terms and conditions apply](#).

FAST TRACK COMMUNICATION

Rotational dynamics of dissociating H_2^+ in a short intense laser pulse

Fatima Anis, Ted Cackowski and B D Esry

J R Macdonald Laboratory, Department of Physics, Kansas State University, Manhattan, KS 66506, USA

Received 30 January 2009

Published 21 April 2009

Online at stacks.iop.org/JPhysB/42/091001**Abstract**

We present a fully quantum mechanical treatment of H_2^+ in intense laser pulses as short as 5 fs, focusing on the rotational dynamics of the dissociating fragments. The dependence of the dynamics on the pulse length and intensity is examined. We find that including nuclear rotation is essential for predicting the angular distribution of fragments even in these very short pulses. We further find that the axial recoil approximation holds for H_2^+ only when the laser pulse is longer than roughly 100 fs.

(Some figures in this article are in colour only in the electronic version)

1. Introduction

The dissociation and ionization of H_2^+ in intense short laser pulses have been extensively studied for almost two decades [1, 2]. Nevertheless, this simple one-electron molecule still has phenomena left to explore and dynamics left to understand. In fact, as laser pulses get shorter, previously studied phenomena need to be re-examined as they form the basis of our physical intuition. That intuition, however, may be underpinned by assumptions—good for long pulses—that fail for short pulses.

In this communication, we examine the dynamics of the angular distribution of H_2^+ dissociating to $p+\text{H}$ in short laser pulses using a fully quantum mechanical approach [3]. In particular, we study the relative importance of dynamic and geometric alignments as a function of the pulse length. Dynamic alignment is the process in which the laser's electric field torques the molecules into alignment along the laser polarization direction before dissociating or ionizing them [1]. Being a light molecule, H_2^+ undergoes greater dynamic alignment than, for instance, I_2 in the same laser pulse [1]. Dynamically aligned dissociating fragments exhibit a narrow angular distribution along the polarization direction [2]. At the opposite end of the dynamical spectrum, geometric alignment refers to the preferential dissociation or ionization of the molecules aligned with the laser polarization. Thus, geometric alignment implies the lack of angular dynamics.

Both dynamic and geometric alignments occur during the laser pulse. The physical observable in experiments,

however, is the angular distribution at the detector—in other words, at infinite times. When interpreting their findings, experimentalists often assume these infinite-time angular distributions are the same as at the moment that the molecule breaks, neglecting any post-pulse rotation of the recoiling fragments [4, 5]. The experimental data analysis does not typically rely on this 'axial recoil approximation' as it is only an interpretive assumption. Nevertheless, this assumption has shaped many people's physical picture of the dynamics of diatomic molecules in intense laser pulses.

Since it does not appear to be a straightforward proposition to experimentally measure post-pulse alignment, even using pump-probe techniques, we must study it theoretically. Thus, another of our goals for this communication is to check the validity of the axial recoil approximation. While its validity has been addressed in previous studies using a classical model [6] and using a semi-classical model combined with rigid rotor quantum mechanical calculations [7–9], a fully quantum mechanical examination has not previously been undertaken.

To address our goals, we performed a comprehensive study of the dynamics of the angular distribution of H_2^+ dissociating in an intense laser pulse for peak intensities from $10^{10} \text{ W cm}^{-2}$ to $10^{14} \text{ W cm}^{-2}$ and pulse lengths ranging from 135 fs to 5 fs. Although all of the pulses in this range are very short compared to the free rotational period of H_2^+ (≈ 556 fs), the angular dynamics both during and after the pulse changes character significantly. We illustrate the importance of nuclear rotation in all cases by comparing the results of our calculations

with and without nuclear rotation. We conclude, perhaps surprisingly, that even for pulses as short as 5 fs it is important to include nuclear rotation in order to obtain accurate angular distributions.

2. Method

As described in [3], we use the time-dependent Born–Oppenheimer representation with nuclear rotation (TDBOR) and the time-dependent Born–Oppenheimer representation with aligned nuclei (TDBOA). As their names imply, both involve the solution of the time-dependent Schrödinger equation with the former including nuclear rotation and the latter not. A detailed description of both methods is presented in [3], so we give only a few important details here.

We first calculated the Born–Oppenheimer potentials and dipole transition matrix elements as described in [10]. In our formulation, we neglected all non-Born–Oppenheimer coupling terms in both methods and the Coriolis coupling terms in the TDBOR. In the TDBOR, nuclear rotation is included via an expansion over Wigner D -functions. The radial degree of freedom is represented on a grid using a generalized finite difference scheme [11] and is propagated using split operator techniques combined with the Crank–Nicolson evaluation of the operator exponentials. For this communication, the key point is that the TDBOR calculations should be essentially exact in the sense that all physical processes and degrees of freedom important in this intensity regime are included. We did neglect ionization, but its contribution is large only at higher intensities which we avoided.

The interaction between the laser and molecule is treated in the dipole approximation using the length gauge. The interaction potential is thus $-\mathcal{E}(t) \cdot \mathbf{d}$, where $\mathcal{E}(t)$ is the linearly polarized electric field and \mathbf{d} is the dipole operator. The pulse envelope for all the calculations is Gaussian, with $\mathcal{E}(t)$ given explicitly as

$$\mathcal{E}(t) = \hat{\mathbf{z}} \mathcal{E}_0 e^{-\frac{t^2}{\tau^2}} \cos(\omega t + \varphi). \quad (1)$$

In (1), \mathcal{E}_0 is the peak electric field in atomic units¹. The parameter τ is related to the full width of the intensity at half maximum τ_{FWHM} by $\tau = \tau_{\text{FWHM}}/\sqrt{2 \ln 2}$. When we refer to a pulse length in the remainder of this communication, we mean τ_{FWHM} . The carrier-envelope phase φ is taken to be equal to zero for all calculations; and ω is the frequency in atomic units corresponding to 785 nm, the central wavelength of a Ti:sapphire laser. Finally, the unit vector $\hat{\mathbf{z}}$ refers to the z -axis in the laboratory frame.

3. Results and discussion

3.1. Dynamics during the pulse

As mentioned in section 1, the dynamics of the angular distribution is generally described by the limits: geometric and dynamic alignments. Defining these phenomena

¹ The laser electric field \mathcal{E}_0 is related to the peak intensity I by $\mathcal{E}_0 = \sqrt{I/(3.5 \times 10^{16} \text{ W cm}^{-2})}$.

quantitatively within the TDBOR (or experimentally) is not a simple task. Fortunately, comparing the TDBOA and TDBOR results for the total dissociation probability P_D has proven to be a useful way to quantify dynamic alignment. This usefulness follows from the fact that the molecule is not allowed to rotate in TDBOA and thus displays purely geometric alignment. The magnitude of the dynamic alignment is thus given by the difference in P_D between the two calculations. Care must be taken when performing this comparison, however, to ensure that the initial angular distribution in the two methods match.

The TDBOR results presented here start from the $J = 0$ state, where J is the total orbital angular momentum. To mimic this initial angular distribution, the TDBOA results must be averaged over the initial angle θ between the internuclear axis and the laser polarization as follows:

$$\bar{P}_D(I) = \frac{\int_0^\pi P_D(I, \theta) \sin \theta d\theta}{\int_0^\pi \sin \theta d\theta}, \quad (2)$$

where I is the peak intensity. Since we consider comparatively low intensities in the TDBOA, the above integral can easily be converted to an intensity integral using the fact that the $1s\sigma_g$ to $2p\sigma_u$ transition provides the dominant contribution to H_2^+ dissociation [1, 2]. This is a parallel, $\Delta\Lambda = 0$, transition that depends only on the component of the laser field along the internuclear axis. We verified that the contribution of perpendicular transitions is indeed negligible by including higher excited electronic states. We can therefore define an effective intensity, $I_{\text{eff}} = I \cos^2 \theta$, so that $P_D(I, \theta) = P_D(I_{\text{eff}}, 0)$. This transforms the above equation to

$$\bar{P}_D(I) = \frac{1}{2} \int_0^I P_D(I_{\text{eff}}, 0) \frac{dI_{\text{eff}}}{\sqrt{I_{\text{eff}} I}}. \quad (3)$$

We have calculated and analysed P_D as a function of peak laser intensity for three pulse lengths—10 fs, 45 fs and 135 fs. For the 45 fs and 135 fs pulses, we used a maximum peak intensity of $10^{13} \text{ W cm}^{-2}$, while for the 10 fs pulse this has been extended to $10^{14} \text{ W cm}^{-2}$. Figure 1 shows the results for initial vibrational states $v = 7, 9$ and 12. Dissociation is dominated by the one-photon, bond-softening transition from $v = 9$. The figure also includes P_D obtained by averaging over the initial vibrational states, each weighted by their Franck–Condon factor from the H_2 ground vibrational state as is appropriate for comparison with ion-beam H_2^+ targets [12].

Figure 1 shows that the disagreement between the TDBOA and TDBOR results grows with the laser peak intensity in every case, indicating the increasing importance of dynamic alignment with intensity—which is expected. What may not have been expected is that dynamic alignment can be significant even for 10 fs pulses, leading to a roughly 10% increase in P_D at $10^{14} \text{ W cm}^{-2}$ compared to purely geometric alignment. This result can be understood from the fact that at higher peak intensities, the pulse spends a much longer time at non-perturbative intensities. A 10 fs, $10^{14} \text{ W cm}^{-2}$ pulse spends roughly 25 fs at intensities above $10^{12} \text{ W cm}^{-2}$. Such exposure is sufficient to drive transitions to the higher angular momentum states needed for the molecule to align, and the time is long enough for some rotation to occur.

Figure 1 also shows that the difference between the TDBOR and TDBOA results grows with the pulse length.

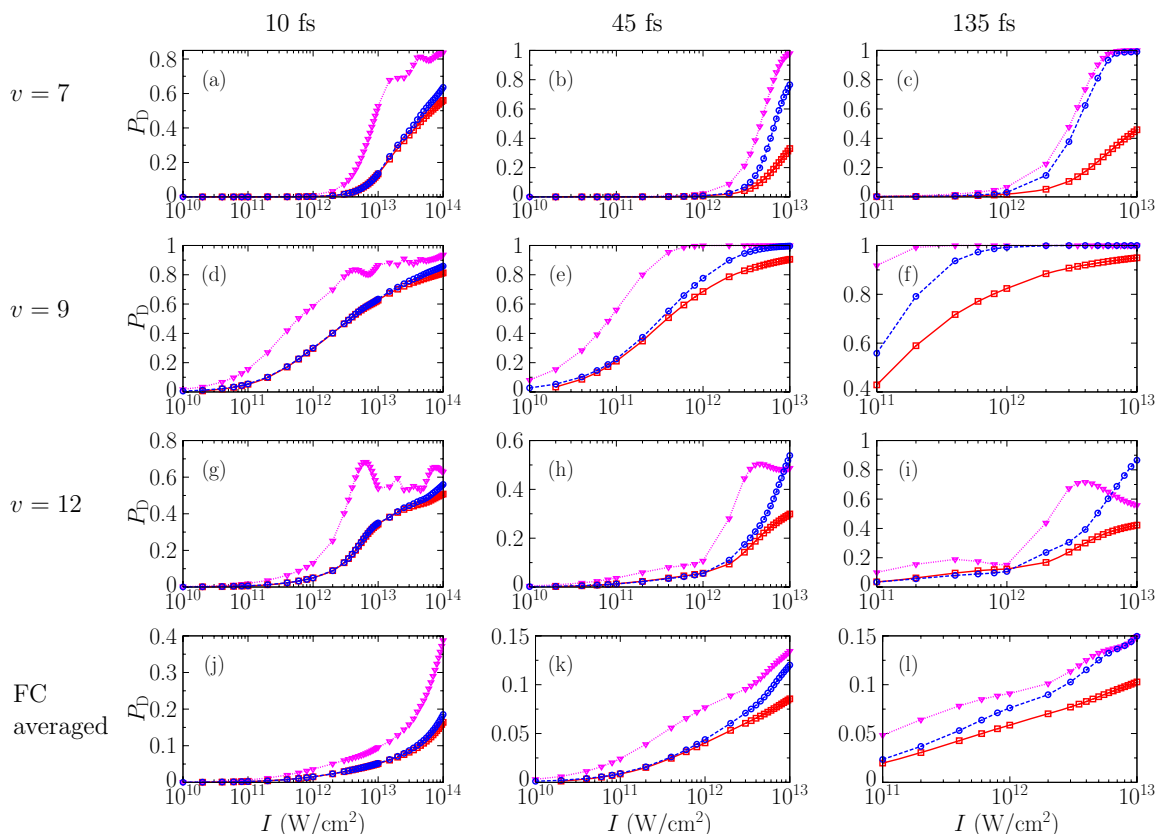


Figure 1. The total dissociation probability in different approximations for pulse lengths 10, 45 and 135 fs and initial vibrational states $v = 7, 9, 12$. The last row presents the dissociation probability averaged over the initial Franck–Condon (FC) vibrational distribution. The red solid lines (\square) show the angle-averaged $P_D(I)$ from TDBOA; the blue dashed lines (\circ), the TDBOR $P_D(I)$; and the magenta dotted lines (∇), the TDBOA $P_D(I, \theta = 0)$. Note that the panels have different scales for clarity.

As the pulse length gets longer in the TDBOR calculations, the field acts for a longer time, allowing for greater dynamic alignment. As the molecule becomes more aligned, it experiences a higher effective intensity and consequently dissociates with greater probability. In the TDBOA, the molecule cannot rotate and the molecule experiences only a fixed effective intensity throughout the pulse. By this argument, the angle-averaged TDBOA results should always underestimate the exact dissociation probability. This conclusion is supported by figure 1 except for $v = 12$ in figure 1(i) at low intensities where the TDBOA results are slightly higher.

Since the vast majority of calculations in the literature for H_2^+ in intense laser pulses are performed for molecules aligned with the laser field without angle averaging or nuclear rotation [1, 2, 12–17], we have also included in figure 1 P_D for $\theta = 0$ from the TDBOA, i.e. without any angle averaging. Because they represent completely aligned molecules, these results should provide an upper limit on P_D since all molecules experience the maximum possible intensity throughout the laser pulse. As such, these $\theta = 0$ TDBOA results can also be regarded as the extreme of dynamic alignment. Figure 1 again bears out these expectations with the exceptions coming now at higher intensities for $v = 12$. The TDBOR results more-or-less interpolate between the angle-averaged TDBOA and the $\theta = 0$ TDBOA results as intensity increases from low to high.

For 10 fs pulses, the angle-averaged TDBOA provides reasonably good quantitative results over much of this intensity range, indicating that dynamic alignment is not playing a substantial role except at the highest intensities. This conclusion is, of course, consistent with the common assumption of no nuclear rotation in a pulse so much shorter than the free rotation period (556 fs for H_2^+). The $\theta = 0$ TDBOA results, however, do not agree with TDBOR for any intensities in this range, and only give reasonable qualitative agreement for the Franck–Condon-averaged P_D .

The angle-averaged TDBOA also gives reasonably good quantitative results for 45 fs pulses, although over a smaller range of intensities than for 10 fs pulses. Moreover, the $\theta = 0$ TDBOA results give a better qualitative answer than for 10 fs, but little better quantitative agreement where the probability is not saturated. The Franck–Condon-averaged TDBOR results, however, do appear to be headed for more quantitative agreement with the $\theta = 0$ TDBOA at higher intensities than can be reliably treated without including ionization.

For 135 fs pulses, the angle-averaged TDBOA is no longer in quantitative agreement with TDBOR for the intensity range studied. In fact, the TDBOR results are in much better quantitative agreement with the $\theta = 0$ TDBOA results, especially at higher intensities for the Franck–Condon-averaged P_D . We conclude, then, that dynamic alignment can be quite important already for 135 fs pulses—which are still

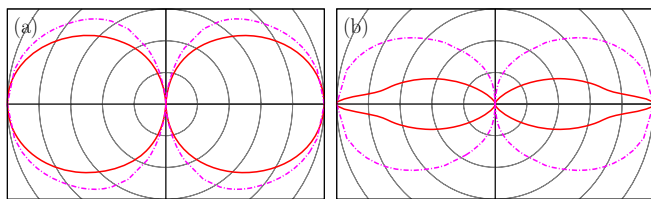


Figure 2. The angular distribution of $p+H$ fragments at t_f for a 10 fs pulse: (a) $I = 10^{13} \text{ W cm}^{-2}$ and (b) $I = 10^{14} \text{ W cm}^{-2}$. The magenta dot-dashed lines show TDBOA results; and the red solid line, TDBOR. The two distributions in each panel have been normalized to have the same maximum value to better show the qualitative comparison. The laser polarization lies along the horizontal axis in these figures.

shorter than the free rotation period. In fact, it was calculations at long pulse lengths similar to these that were originally used to justify using the $\theta = 0$ TDBOA calculations to *qualitatively* understand the dynamics of H_2^+ in an intense field [2]. We see from figure 1, though, that the $\theta = 0$ TDBOA calculations fail to provide a good qualitative description for most of the cases shown. The greatest discrepancies appear for the initial vibrational states at the shortest pulse lengths. Incidentally, we note that angle averaging the TDBOA results eliminates the stabilization (decrease in P_D with intensity) seen in the $\theta = 0$ TDBOA curves for $v = 12$. It has already been noted that inclusion of nuclear rotation largely eliminates this vibrational trapping [3, 15, 16, 18], but it is interesting that angle averaging does as well.

The comparison in figure 1 between the TDBOR and the angle-averaged TDBOA P_D shows that for moderate intensities, the angle-averaged TDBOA calculations actually give fairly accurate results for the shorter laser pulses. This finding is attractive as the TDBOA calculations are much faster than the TDBOR, even when several intensities need to be calculated to carry out the angle averaging via (3). On the other hand, if more detailed information such as the angular distribution is desired, then the predictive power of the TDBOA degrades quickly. Figure 2 shows the Franck–Condon-averaged $P_D(I, \theta)$ for a 10 fs pulse from both calculations at the end of the laser pulse t_f (defined as the time at which the intensity decays to 10^6 W cm^{-2}). The distributions in figure 2(a) for $10^{13} \text{ W cm}^{-2}$, where the total dissociation probabilities in figure 1 agree quite well, are similar, although not in quantitative agreement. Those in figure 2(b) for $10^{14} \text{ W cm}^{-2}$, however, show distinct differences even though the total dissociation probabilities show only about a 25% relative difference.

3.2. Dynamics after the pulse

We have already shown surprising consequences of nuclear rotation on the dissociation probability and the angular distribution at the end of the laser pulse for pulses much shorter than the free rotation period. But, as mentioned previously, this distribution is not physically observable. To obtain the observable, we must extract the angular distribution from the calculations at infinite time. Since the discussion here will focus on the role of nuclear rotation in the system's

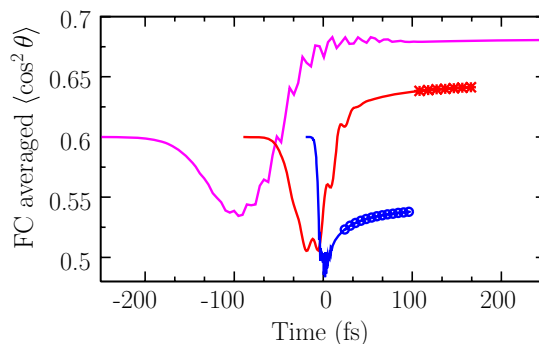


Figure 3. Franck–Condon-averaged $\langle \cos^2 \theta \rangle$ during the pulse (no symbols) and after the pulse (symbols) for 10 fs (blue \circ), 45 fs (red $*$) and 135 fs (magenta) pulses at $I = 10^{13} \text{ W cm}^{-2}$.

evolution from the end of the pulse to infinity—and thus on the validity of the axial recoil approximation—the remainder of this communication will be based only on the TDBOR results.

In addition to the angular distribution itself, one quantity commonly used to parametrize the alignment of a molecule is $\langle \cos^2 \theta \rangle$, which is related to the width of the angular distribution for a homonuclear diatomic molecule. Normally, it is the alignment of the bound molecule that is characterized by $\langle \cos^2 \theta \rangle$, but we will use it here to help us understand the angular evolution of the dissociating fragments. Figure 3 shows the Franck–Condon-averaged $\langle \cos^2 \theta \rangle$ for only the dissociating part of the wavefunction. The averaging is defined as

$$\langle \cos^2 \theta \rangle = \frac{\sum_v f_v \langle \cos^2 \theta \rangle_v}{\sum_v f_v P_{Dv}}, \quad (4)$$

where the subscript v indicates the initial vibrational state, P_{Dv} the total dissociation probability for v and f_v is the Franck–Condon factor. The quantity $\langle \cos^2 \theta \rangle_v$ in (4) is calculated with the time-dependent wavefunction that has had all of the time-independent, bound rovibrational states projected out. The initial value of $\langle \cos^2 \theta \rangle$ for all three pulses is 0.6—a consequence of the fact that dissociation from $J = 0$ requires absorption of at least one photon and $\langle \cos^2 \theta \rangle = 0.6$ for $J = 1$. This result holds for low intensity calculations with only two channels, and may change after including the π states for high laser intensities. We note that this figure also supports the discussion of the previous section, showing that the angular distribution of the fragments starts changing at times early compared to the pulse length. For instance, $\langle \cos^2 \theta \rangle$ for 45 fs has reached its first extreme already at about 20 fs before the peak intensity.

Key to the present discussion is the post-pulse behaviour of $\langle \cos^2 \theta \rangle$. We define the time t_f at which the pulse intensity decays to 10^6 W cm^{-2} as the end of the pulse, so that all subsequent evolution is effectively field free and considered post-pulse. We note that by this definition, the time range in figure 3 spans times up to t_f for the 135 fs pulse. Towards the end of the pulse, $\langle \cos^2 \theta \rangle$ for the 135 fs pulse has already obtained its asymptotic value, implying that the axial recoil approximation works quite well for 135 fs or longer pulses. In contrast, $\langle \cos^2 \theta \rangle$ for both 45 and 10 fs pulses continues to change towards the end of pulse and after.

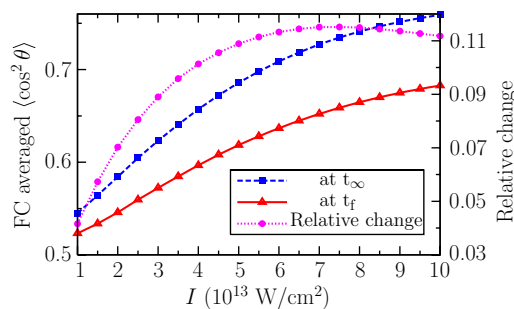
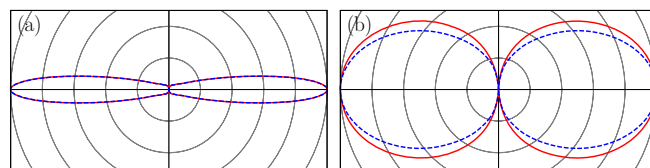
Table 1. Franck–Condon-averaged $\langle \cos^2 \theta \rangle$ from TDBOR for $I = 10^{13} \text{ W cm}^{-2}$.

FWHM (fs)	$\langle \cos^2 \theta \rangle$		Relative change (%)
	at t_f	at $t \rightarrow \infty$	
135	0.681	0.683	0.3
45	0.640	0.648	1.2
10	0.523	0.545	4.2

We can understand the behaviour displayed in figure 3 in exactly the same way that the alignment of bound states by intense laser pulses is understood [21]. In that case, there are two limits: impulsive alignment when the pulse is much shorter than the free rotation period, and adiabatic alignment when the pulse is much longer. The mechanism of impulsive alignment is the generation of a distribution of angular momentum states by the laser pulse that do not have time to evolve during the short pulse. There is thus no alignment during the pulse, but the distribution continues to evolve freely after the pulse ends, leading to periodic revivals during which the molecules are maximally aligned. In a long laser pulse, molecules adiabatically align because the field-free states adiabatically correlate to pendular states in the field—the lowest of which is strongly aligned. The pendular states also involve a broad distribution of angular momentum states, but in a long pulse, they have time to evolve into a narrow angular distribution.

Given these two alignment mechanisms, we see from the behaviour in figure 3 that the 10 fs and 45 fs data are explained by impulsive alignment, demonstrating that this mechanism works for the dissociating fragments as well as for the bound components. Because the dissociating component has acquired a broad angular momentum distribution similar to the bound component, it continues to evolve after the pulse, becoming more aligned on the way to the detector. There are no revivals for the dissociating component since its moment of inertia grows as the fragments separate, effectively freezing the angular distribution as the fragments fly to the detector. The 135 fs data, on the other hand, are explained by adiabatic alignment. When the molecule becomes aligned near the peak intensity of the pulse, it dissociates. Because it was in a pendular (or near-pendular) state, its angular distribution did not evolve further.

To quantify the post-pulse alignment, we have calculated $\langle \cos^2 \theta \rangle$ at infinite time. Two ways to do this are to continue propagating the dissociating part of the wavefunction to very large times, or by writing the wavefunction at the end of the pulse in terms of the exact scattering states, superposed to give outgoing plane waves at large internuclear distances [2, 19]. The former scheme is not very practical and involves extensive computational work. Therefore, we adopted the latter scheme, but doublechecked it for one pulse length with the former to confirm that they converged to the same answer at very large times. Table 1 shows the results for the three pulses of figure 3, and the results are consistent with that figure. For the 135 fs pulse, the angular distribution is more aligned than both the 45 and 10 fs pulses, but it barely changes on its way

**Figure 4.** Franck–Condon-averaged $\langle \cos^2 \theta \rangle$ from TDBOR at the end of the pulse (t_f) and at the detector ($t \rightarrow \infty$) for a 10 fs pulse.**Figure 5.** Franck–Condon-averaged TDBOR angular distribution for dissociation in (a) 135 and (b) 10 fs pulses at $I = 10^{13} \text{ W cm}^{-2}$. Red solid lines denote distribution at t_f ; and blue dashed lines, at $t \rightarrow \infty$.

to the detector. The shorter pulses are less aligned, but have much larger relative change in $\langle \cos^2 \theta \rangle$ after the pulse.

One natural question is: can the relative change in $\langle \cos^2 \theta \rangle$ after the pulse be larger than the 4% found for the 10 fs pulse? To answer this question, we studied the dependence of the post-pulse alignment on laser peak intensity for the 10 fs laser pulse. Figure 4 shows the results. In fact, the relative change grows by about a factor of three to a maximum of about 11% as the peak intensity is raised from $10^{13} \text{ W cm}^{-2}$. From figure 4, we see that the values of $\langle \cos^2 \theta \rangle$ at t_f and $t \rightarrow \infty$ both increase monotonically with intensity. It has already been mentioned, however, in previous section that higher intensities mean longer pulse duration above perturbative intensities and consequently large dynamic alignment during the pulse, implying that relative change of $\langle \cos^2 \theta \rangle$ should therefore have a maximum and become gradually smaller with increasing intensity. It appears that we have located this maximum value at a laser peak intensity of $7 \times 10^{13} \text{ W cm}^{-2}$. Of course, at higher intensities, the competing process of ionization will become increasingly important, and we do not know what its impact will be. We can conclude, though, that the axial recoil approximation is breaking down for dissociation of H_2^+ in 10 fs laser pulses.

To better visualize the post-pulse alignment, it helps to study the full angular distributions rather than just their width via $\langle \cos^2 \theta \rangle$. So, we show in figure 5 angular distributions at t_f and $t \rightarrow \infty$ for $10^{13} \text{ W cm}^{-2}$. It is evident from figure 5(a) that the fragments from dissociating H_2^+ in a 135 fs laser come out very aligned and do not rotate appreciably as they head towards the detector. The 10 fs distribution in figure 5(b), whose $\langle \cos^2 \theta \rangle$ increased by 4% after the pulse, does show visible post-pulse narrowing.

Qualitatively, the t_f and $t \rightarrow \infty$ distributions in figure 5 are similar, even for the 10 fs pulse. Is it possible, then, to find

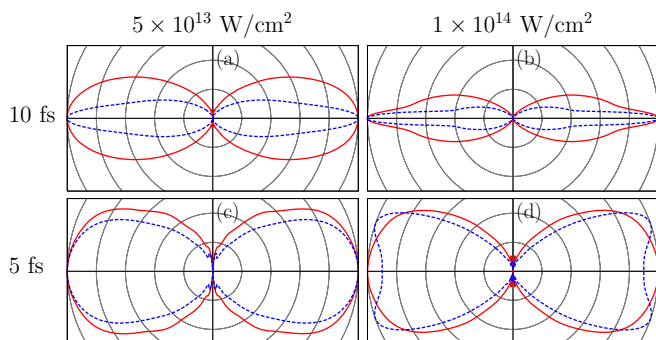


Figure 6. Franck-Condon-averaged TDBOR angular distribution for dissociation. Red solid lines denote distribution at t_f ; and blue dashed lines, at $t \rightarrow \infty$.

qualitatively different t_f and $t \rightarrow \infty$ angular distributions? The answer is yes, and a few examples are shown in figure 6. Figure 6(a) and 6(b) compare the distributions for a 10 fs pulse at these two times for higher intensities where the effect is more dramatic as is suggested by figure 4. If the t_f and $t \rightarrow \infty$ angular distributions were both experimentally measurable, it would certainly be possible to distinguish them. Even more dramatic is the comparison between figure 6(b) and figure 2(b). The red curve in both cases is the same, showing that the TDBOA calculations certainly cannot be used to predict the angular distributions at the detector for $10^{14} \text{ W cm}^{-2}$.

We also compare in figure 6 the results for a 5 fs laser pulse to see if nuclear rotation could possibly be important for such a short pulses. Note that although the physical observables generally show some dependence on the carrier-envelope phase for such short pulses [20], we show results only for zero carrier-envelope phase. For comparison, $\langle \cos^2 \theta \rangle$ for figures 6(c) and (d) at t_f is 0.531 and 0.576, respectively. While these values are smaller than for the corresponding 10 fs angular distributions, the relative post-pulse changes in $\langle \cos^2 \theta \rangle$ of 10.5% and 12.3%, respectively, are higher than for the 10 fs pulse, continuing the trend already observed. Figure 6 shows, however, that their post-pulse evolution is quite different and that the angular distribution does not look as sharply aligned. Moreover, a structure has developed in the angular distribution in figure 6(d).

4. Summary

We have studied the dynamics of the angular distribution of $p+H$ fragments following the intense field dissociation of H_2^+ both during and after the laser pulse. We found significant dynamic alignment during 135 fs pulses, but little rotation after

the pulse. We also found that geometric alignment dominates during 10 fs pulses of moderate intensity, but the molecules can rotate considerably after the pulse. Consequently, the axial recoil approximation appears to hold best for pulses on the order of 135 fs or longer. Also consequently—and in contrast to the assumptions in most work in this field—nuclear rotation must be included to correctly predict even the qualitative features of the angular distribution of H_2^+ dissociation in short pulses.

Acknowledgments

We gratefully acknowledge the suggestion by A Saenz to perform the angular average for the aligned model calculations. The work was supported by the Chemical Sciences, Geo-Sciences, and Biosciences Division, Office of Basic Energy Sciences, Office of Science, US Department of Energy.

References

- [1] Posthumus J H 2004 *Rep. Prog. Phys.* **67** 623 (and references therein)
- [2] Giusti-Suzor A, Mies F H, DiMauro L F, Charron E and Yang B 1995 *J. Phys. B: At. Mol. Opt. Phys.* **28** 309–39 (and references therein)
- [3] Anis F and Esry B D 2008 *Phys. Rev. A* **77** 033416
- [4] Zare R N 1967 *J. Chem. Phys.* **47** 204
- [5] Siebbeles L D A, Glass-Maujean M and Vasyutinskii O S 1994 *J. Chem. Phys.* **100** 3610
- [6] Wood R M, Zheng Q, Edwards A K and Mangan M A 1997 *Rev. Sci. Instrum.* **68** 1382
- [7] Zheng Q, Edwards A K, Wood R M and Mangan M A 1995 *Phys. Rev. A* **52** 3945
- [8] Kuznetsov V V and Vasyutinskii O S 2005 *J. Chem. Phys.* **123** 034307
- [9] Tong X M, Zhao Z X, Alnaser A S, Voss S, Cocke C L and Lin C D 2005 *J. Phys. B: At. Mol. Opt. Phys.* **38** 333
- [10] Esry B D and Sadeghpour H R 1999 *Phys. Rev. A* **60** 3604
- [11] Bromley M W J and Esry B D 2004 *Phys. Rev. A* **69** 053620
- [12] Wang P Q, Saylor A M, Carnes K D, Xia J F, Smith M A, Esry B D and Ben-Itzhak I 2005 *Phys. Rev. Lett.* **95** 073002
- [13] Chelkowski S, Zuo T, Atabek O and Bandrauk A D 1995 *Phys. Rev. A* **52** 2977
- [14] Atabek O and Lefebvre R 2008 *Phys. Rev. A* **78** 043419 (and references therein)
- [15] Giusti-Suzor A and Mies F H 1994 *Phys. Rev. Lett.* **68** 3869
- [16] Aubanel E E, Gauthier J-M and Bandrauk A D 1993 *Phys. Rev. A* **48** 2145
- [17] Hua J J and Esry B D 2008 *Phys. Rev. A* **78** 055403
- [18] Aubanel E E, Conjusteau A and Bandrauk A D 1993 *Phys. Rev. A* **48** R4011
- [19] Charron E, Giusti-Suzor A and Mies F H 1994 *Phys. Rev. A* **49** R641
- [20] Roudnev V and Esry B D 2007 *Phys. Rev. Lett.* **99** 220406
- [21] Stapelfeldt H and Seideman T 2003 *Rev. Mod. Phys.* **75** 543